Article:
Haque, N and Mullis, AM orcid.org/0000-0002-5215-9959 (2019) Order–Disorder Morphologies in Rapidly Solidified Ni3Ge Intermetallic. JOM, 71 (8). pp. 2728-2733. ISSN 1047-4838

https://doi.org/10.1007/s11837-019-03587-5

Order-disorder morphologies in rapidly solidified Ni_3Ge intermetallic

Nafisul Haque[1, 2], Andrew M. Mullis[1]

[1] School of Chemical & Process Engineering, University of Leeds, Leeds LS2 9JT, UK

[2] Department of Metallurgical Engineering, NEDUET, University Road, Karachi 75270, Pakistan

[a] Corresponding author: engrnafis@gmail.com, A.M.Mullis@leeds.ac.uk

Keywords: rapid solidification; intermetallic compound; microstructure and order-disorder

Abstract

Congruently melting intermetallic, single-phase Ni_3Ge (T_m = 1132°C) has been rapidly solidified via drop-tube processing wherein powders, with diameters between ≥ 850 to ≤ 38 μm, with equivalent cooling rates of ≤ 700 to > 54500 K s^{-1}, were produced. Six dominant solidification morphologies were identified with increasing cooling rate, explicitly; (i) spherulites, (ii) mixed spherulites & dendrites, (iii) dendrites - orthogonal, (iv) dendrites - non-orthogonal, (v) recrystallized, and (vi) dendritic seaweed, are observed imbedded within a featureless matrix. Selected area diffraction (SAD) in the transmission electron microscope (TEM) analysis confirmed that it is only the spherulite microstructure that is partially ordered amongst the above listed microstructures, which are disordered. However, SAD analysis indicated that the featureless background material of all above microstructures is chemically ordered. Thermal analysis indicates a non-reversible reaction.

Introduction

Dendrites are one of the most common morphologies observed during the solidification of metallic materials. In contrast spherulites, although common in polymers, are rare in metals, particularly during single-phase solidification. In polymers, spherulites are most common during the crystallization of high molecular weight melts, where topological constraints restrict the reorientation of long chain molecules [1]. This basic physics was used by Granasy *et al*. [2] to construct a phase-field model of spherulite growth, the fundamental ingredient of which was that translational diffusion was significantly easier than rotational diffusion.

Despite this, spherulites are known to occur in some simple systems where rotational diffusion would not normally be considered to be restricted. One such example is elemental selenium, although the formation of spherulites has been more commonly reported in the course of devitrification of amorphous metals when held above the glass transition temperature. Metallic glass systems in which spherulites have been observed upon devitrification include Ni-P [3], Fe-Si-B [4], Zr-Cu-Al [5, 6] and Zr-Cu-Ni-Al-Nb [7-9]. In a laser processing study on the Zr-Cu-Ni-Al-Nb system [9] found that spherulites form at the same composition as the amorphous matrix, concluding that under such conditions the formation of spherulites was a growth dominated process.

Some common requirements for the formation of spherulites are known despite disagreement regarding the formation mechanism for their growth. One requirement is a disposition to non-crystallographic orientations by means of small angle branching [10]. Another requirement is that a high viscosity should exist in the medium in which crystallization occurs. Morse *et al*. [11] showed the importance of this second requirement by examining the crystallization behavior of approximately seventy inorganic salts in media of varying viscosity. This high viscosity of the crystallizing media presumably accounts for why spherulites are relatively common during the crystallization of amorphous metals.

In this paper we will explore the relatively uncommon phenomenon of spherulite formation during crystallization from a metallic melt. The particular system we will investigate in this respect is the intermetallic compound β-Ni_3Ge. Under equilibrium solidification conditions β-Ni_3Ge will solidify with the ordered $L1_2$ crystal structure at all temperatures below the liquidus. However, it has been shown that for undercoolings in excess of 168 K, corresponding to a critical growth velocity of 0.22 m s^{-1}, complete disorder trapping occurs [12].

Moreover, not only can β-Ni_3Ge be made to crystalize to a spherulitic morphology, but by changing the solidification conditions the spherulitic morphology will transform into different microstructures namely, mixed spherulites & dendrites, dendrites-orthogonal, dendrites-non-orthogonal, recrystallized, and dendritic seaweed. As such, β-Ni_3Ge is an interesting compound in which to study the fundamental dynamics of microstructure formation in a single-phase material. Due to the importance of order-disorder reactions in the formation of microstructure in β-Ni_3Ge, we also performed Differential scanning calorimetry (DSC) on the

rapidly solidified material, in order to identify whether the ordering reaction giving rise to spherulite formation is reversible or irreversible.

Experimental Methods

Congruently melting, single phase β-Ni_3Ge (22.5 to 25.6 at. % Ge) [12] was made by arc melt. To verify that the final compound is homogenous, the process of arc-melting was performed 8 times. An X-ray diffraction (XRD) with a PANalytical Xpert Pro was used to confirm the phase composition of the ingot thus formed. Rapid solidification processing was undertaken using the Leeds 6.5 m drop-tube [13].

The arc-melt ingot, 9.6 g in mass, was loaded into an alumina crucible with three 300 μm laser drilled holes in the base. Induction heating was used to melt the sample with efficient RF coupling being achieved by using a graphite susceptor. Once the desired temperature of 1480 K (1207 °C) (equivalent to 75 K superheat) was achieved the crucible was pressurized to 400 kPa, wherein a spray of fine droplets is produced. These solidify in free fall down the tube, which is maintained at a pressure of 50 kPa. In both cases the gas used was dried, oxygen free N_2. The drop-tube method is explained in detail in [13].

The Ni_3Ge drop-tube powders were prepared for analysis by mounting, grinding, polishing and etching. First, the sieving into particle size ranges of the powders was performed. This was done by utilizing nine wire mesh stacking sieves that have apertures that decrease from ≥ 850 μm (< 700 K s^{-1}) to ≤ 38 μm (> 54500 K s^{-1}). Once loaded with powder the entire stack was actively agitated for 10 minutes. The methodology for the estimation of sample cooling rate is outlined in [14]. The mounting of the powder in a TransOptic™ resin followed from its removal from the sieves.

XRD analysis was used to confirm that the drop-tube powders remained single-phase following rapid solidification processing. Subsequent to XRD analysis they were mounted and polished to a 0.5 μm surface finish for microstructural analysis. After having been polished, the etching of the samples occurred with an equimolar mixture of hydrofluoric, hydrochloric and nitric acids. In order to obtain the microstructure of the droplets exposed by the etching, scanning electron microscope (SEM) imaging was utilized using a Carl Zeiss EVO MA15 SEM. EDX line scans, using a X-Max Oxford instrument Energy-Dispersive X-Ray (EDX) detector on the SEM, were used to investigate any chemical variation across the microstructural features observed after etching. Thermal analysis was used to determine the

reordering transition temperature in the Ni_3Ge compound, with the temperature scan range being from room temperature to 1030 ˚C, at 10 K/min heating/cooling rate in N_2 gas.

Results

In Figure 1, it is shown that XRD peaks from all drop-tube samples may be indexed to β-Ni_3Ge via the ICCD pattern 04-004-3112. When Ahmad et al. [15] deeply undercooled a similar material using a melt fluxing technique, the resultant material also remained single phase. The XRD results here show that the same is valid for rapid cooling via drop-tube processing. Note that here, and throughout the paper, we use the designation β to refer to the chemical phase Ni_3Ge irrespective of whether this is fully ordered ($L1_2$), completely disordered (A1-fcc) or has some intermediate degree of partial chemical ordering.

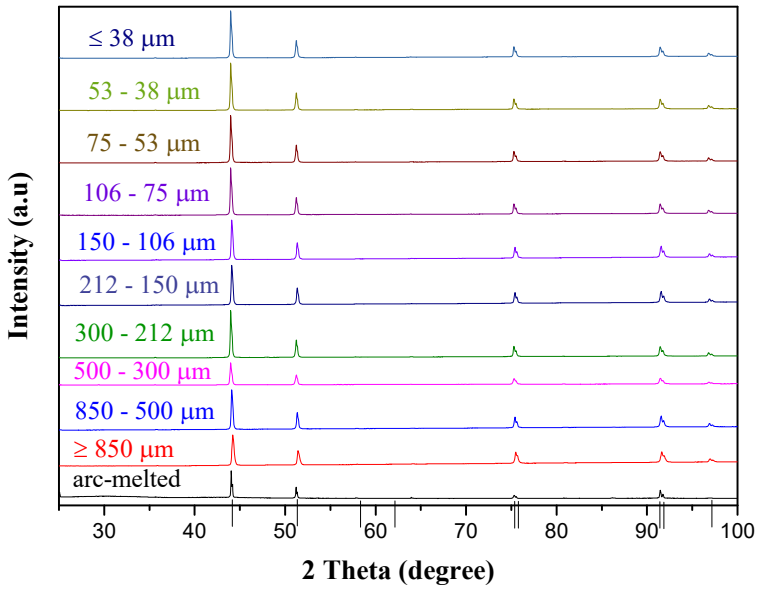

Figure 1: XRD results of an arc melted (black) and rapidly solidified samples, ranges from (≥ 850 µm to ≤ 38 µm) indicating with different colour respectively. Vertical black lines indicate peaks position for the single-phase β-Ni_3Ge reference pattern and different colours represents XRD patterns of particle sizes from ≥ 850 µm to ≤ 38 µm.

EDX analysis was carried out on freshly polished samples to ensure the chemical composition of the all drop-tube samples. For this, EDX area scanning was randomly performed at least on 10 particles of all ranges of drop-tube samples (≥ 850 µm to ≤ 38 µm) with the measured chemical compositions being within the Ni_3Ge homogeneity range Ni –

23.8 at. % Ge as shown in **Figure 2**. Consequently, all ranges of drop-tube particles consists of an average chemical composition within the range of single phase, congruently melting compound, β-Ni_3Ge [16].

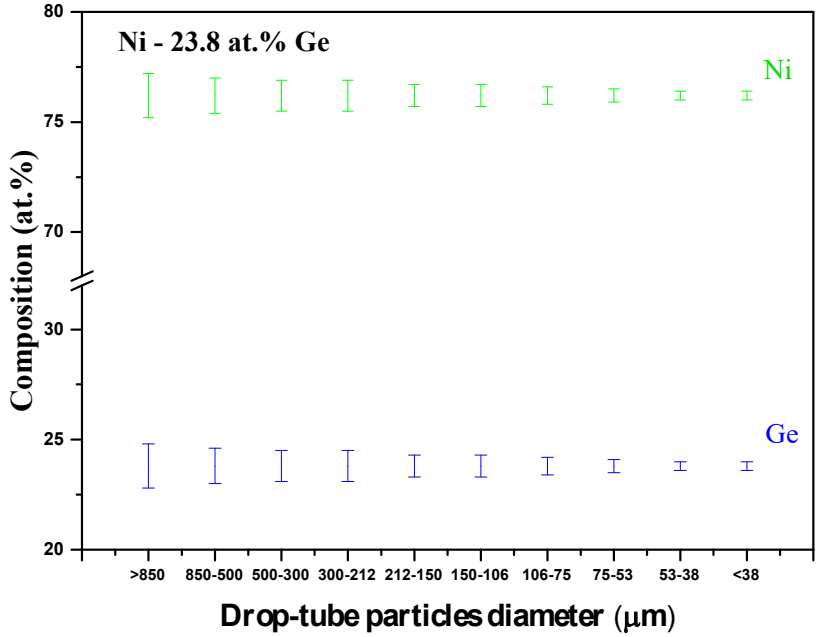

Figure 2: An averaged out EDX concentrations of Ni and Ge (Ni-23.8 at. % Ge) drop-tube samples.

SEM was used for studying microstructures of the rapidly solidified Ni_3Ge droplets. There were six typical microstructures observed, namely (a) Spherulites, (b) mixed spherulites & dendrites (c) dendrites - orthogonal (d) dendrites - non-orthogonal, (e) crack-like (recrystallized), and (f) dendritic seaweed, all of which were observed embedded within a featureless matrix. Typical examples of these microstructures can be seen from the **Figures 3.**

Figure 3a is a typical SEM image from the ≥ 850 μm size fraction. In what is otherwise a featureless matrix, a number of spherulite like structures, which characteristically have diameters within 10-20 μm, are evident. These features appear to be omnipresent in the drop-tube powders in this size fraction. This is also the case in the 850-500 μm size fraction in which the spherulite like structures are smaller, with typical diameters of ≤ 10 μm. Spherulitic structures are also observed in the size range 500-300 μm. However, these are now characteristically ≤ 3 μm in diameter. For the 300-212 μm and 212-150 μm size fractions dendrites and spherulites are observed to co-exist, (Figure 3b), with the proportion of dendrites increasing in the powders from the smaller sieve fraction.

With further reductions in the size of the powder (150-106 μm), spherulites cease to be seen in the microstructure of the etched droplets, with dendrites (orthogonal) become the dominant structure. Figure 3c shows examples of this. When the size of the sample decreases to 75 μm, dendrites are still the dominant morphology evident in the powders, although now these tend to display non-orthogonal side-branching (Figure 3d). With a yet further reduction in droplet size to 75 – 53 μm, numerous crack-like features are apparent as shown in Figure 3e. These features are not however cracks, as this morphology is not observed prior to etching. It is shown in [15] that the crack-like relief is indicative of a recrystallization.

Finally, in the two smallest size fractions 53 – 38 μm and ≤ 38 μm, yet another structure is observed, which might be define a being 'dense branched fractal' or 'dendritic seaweed' in nature, an example of which can be seen in the Figure 3f.

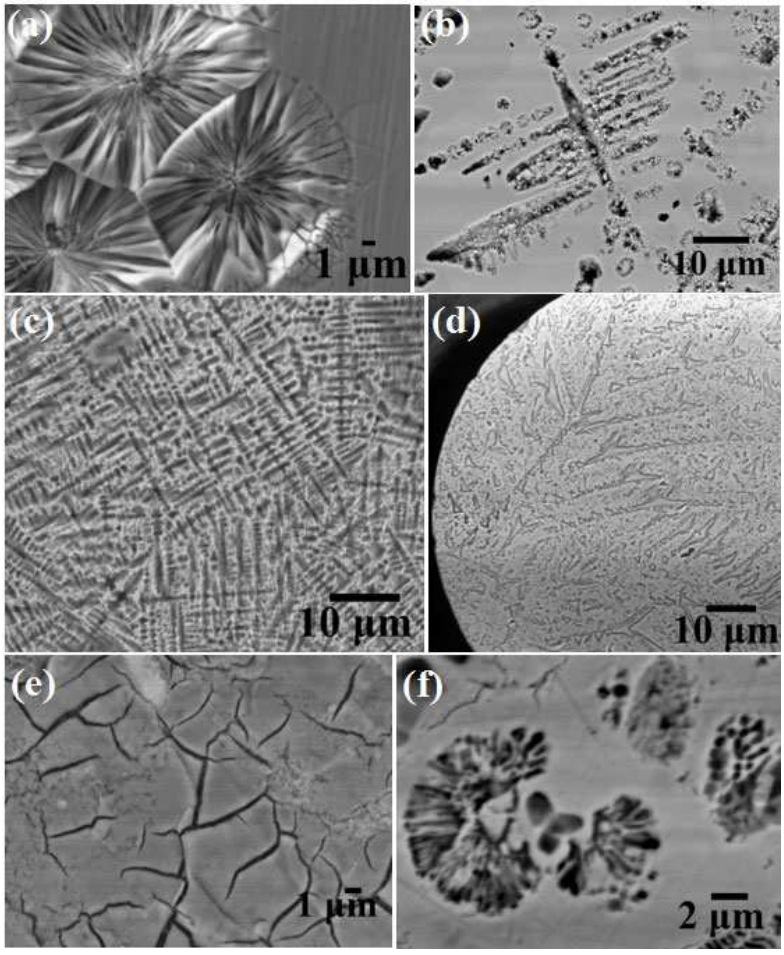

Figure 3: SEM micrograph of hydrofluoric (HF) etched Ni_3Ge drop-tube samples (a) Spherulites, (b) mixed spherulites & dendrites (c) dendrites – orthogonal (d) dendrites - non-orthogonal, (e) crack-like (recrystallized), and (f) dendritic seaweed, are observed imbedded within a featureless matrix.

The microstructures observed in β-Ni_3Ge powders are remarkable for a number of reasons:

1) Spherulites are extremely rare in metallic systems and, as far as we are aware, have never been reported in intermetallics.

2) It is highly unusual to obtain such strong differential etching in a single-phase material, i.e. what has caused some regions to etch and other not to do so. EDX area and line scan measurements confirm that this is not chemical segregation, both regions shown in **Figure 3a** having no detectable chemical inhomogeneity.

3) It is unusual in a fully crystalline material to see such clearly delineated structures. Normally, in for instance a dendritic structure, the intergrowth of differently oriented crystals results in a complex as-solidified microstructure. Here, apparently isolated crystals have grown. Such structures are common in amorphous-crystalline composites, but highly unusual in fully crystalline materials, although the XRD patterns for the drop-tube powders show no evidence for amorphous material in any size fraction. In fact, we have shown in [14] that the contrast arises due to disorder trapping during the recalescence phase of solidification.

DSC analysis was undertaken on the rapidly solidified Ni_3Ge (spherulite samples) with heating rate 10 K min^{-1}, in order to identify any reordering transitions in this system are whether they are reversible or irreversible. The results of this experiment are given in the **Figure 4**, with the DSC trace from the first and second heating/cooling cycle indicated by green & purple arrows respectively. Two vertical black lines indicate potential transition temperatures at 530 to 740 °C. We note that there is generally a close correspondence between the curves for the first and second cycles for both heating and cooling. This is indicative of low drift in the instrument between cycles, giving us confidence in the results and indicates that the material has the same heat capacity in cycle 2 as in cycle 1, whereby the material remains Ni_3Ge. There are two small exothermic (downward) peaks at the indicated temperatures during the first heating cycle, which would be consistent with reordering of the partially disordered material due to disorder trapping during rapid solidification. As these appear only during the first heating cycle this reaction appears irreversible, which is consistent with the ordered variant being more stable than the disordered form at all temperatures below the liquidus. The ordering reaction is discussed in more detail later.

Discussion

A reliable description of the solidification dynamics of Ni_3Ge can be assembled from the SEM, TEM [13, 17, 18] and XRD data. It is clear that all samples are single-phase β-Ni_3Ge, with all XRD peaks being matched to ICCD pattern 04-004-3112. We postulate that the rapidly solidified material formed during recalescence grows as the disordered variant of the material while during slower growth in the post-recalescence phase of solidification the ordered variant is formed. During etching the disordered material is preferentially attacked, revealing the recalescence solidification morphology, which is, depending upon cooling rate, variously spherulitic, dendritic, recrystallized or dendritic seaweed. The more usually found chemically ordered variant is the 'featureless' matrix material, which appear to resist even the very aggressive etchant used here. This is consistent with the chemically resistant nature of intermetallic compounds. The results are in line with TEM results. These show that superlattice spots are found in the material of 'featureless' matrix. However, they are not observed in the orthogonal dendrites, the non-orthogonal dendrites or the dendritic seaweed.

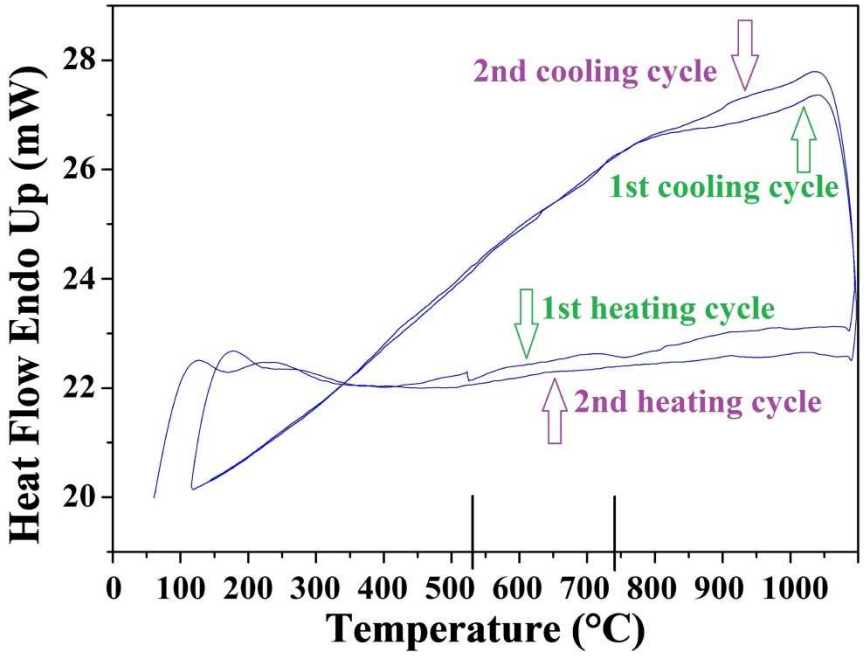

Figure 4: DSC trace from a Ni_3Ge intermetallic compound, first and second heating/cooling cycle indicated by green & purple arrow correspondingly.

For the spherulite morphology the TEM evidence is that the 'featureless' matrix is, as per the other morphologies, fully ordered, but the spherulites themselves are only partially disordered, consisting of alternating filaments of ordered and disordered material. The relationship between undercooling and chemical ordering was explored in detail for the

Ni_3Ge compound by Ahmad *et al*. [19], with it being determined the fully disordered growth occurred for $\Delta T > 168$ K, this being evident by a rapid increase in growth velocity with undercooling above $\Delta T = 168$ K. Unfortunately, direct measurement of undercooling during drop-tube processing is not possible, although it would be expected that smaller droplets would experience higher undercooling, both because of their higher cooling rate and because of the melt sub-division effect. These effects have been quantified by Wang & Wei [19] for drop-tube processed melts and their model estimates that the droplet size required to attain a critical undercooling of $\Delta T > 168$ K is $d < 280$ μm. This is however a maximum undercooling that would be expected in such sized droplets, with the stochastic nature of nucleation meaning that some droplets of this diameter will undercool by much less.

This model, together with the observations of Ahmad *et al*. [19], allow for a consistent explanation of the observed spherulite-dendrite transition observed in the drop-tube samples. For droplets in the size range 850-300 μm the undercooling achieved is < 168 K and the growth during the recalescence phase of solidification is to a partially disordered (mixed ordered/disordered) spherulite morphology. This is also in line with the finding that with decreasing particle size (increasing undercooling), the volume fraction of spherulites increases. For smaller droplets, in the size range 300-150 μm, some droplets achieve an undercooling above 168 K, some do not, and mixed dendrite/spherulite morphologies may be observed. Such mixed morphologies may also be observed in single droplets if the initial undercooling were only marginally above 168 K, as warming of the droplet during recalescence will lower the undercooling. Finally, for droplets with $d < 150$ μm, for which the model of Wang & Wei [19] predicts a maximum undercooling of 270 K, we propose that virtually all droplets achieve an undercooling of at least 168 K and spherulite morphologies cease to be observed.

The dominance of spherulite growth at low undercooling is probably related to the slow, kinetically limited, growth of the ordered phase. The occurrence of spherulites in devitrified metallic glass systems is instructive. The principal difference between crystallization from the melt and crystallization from a metallic glass precursor, is that in a metallic glass the viscosity is much higher and consequently the atomic diffusivity is much lower. As a result, diffusion in a glass is generally restricted to short range such that the atom rearrangement occurs without bulk solute redistribution. In turn this means that the growth rate is limited by kinetics, rather than by diffusion. An isotropic material under pure kinetically limited growth would grow as a sphere [8]. However, crystalline anisotropy within the growing sphere will

favor certain crystal orientations, giving rise to the fine needle spherulite morphology. In the growth of β-Ni_3Ge from its parent melt, a similar condition occurs. There is no need for long-range solute mobility by diffusion since the compound is congruently melting. This is in line with EDX measurements. These show that, within experimental uncertainty, spherulitic and dendritic chemical composition is the same as that of the surrounding matrix material.

Once fully disordered growth is achieved at higher undercooling, there is a switch to a dendritic morphology as growth of the disordered solid is rate limited by diffusion rather than kinetics. With decreasing droplet size (increase of the undercooling) these are observed to switch from having orthogonal to non-orthogonal side-branching. In a cubic system this is characteristic of a switch in the primary growth direction. Typically, cubic systems grow along the <100> directions at equilibrium, with a switch to either <110> or <111> growth being noted at elevated undercooling in a number of systems [20]. A similar change has been observed as precursor to the transition to the dendritic seaweed morphology [21, 22].

From the discussion above it is clear that chemical ordering, and disorder trapping at elevated growth velocity, play a key role in the formation of the observed microstructures. Heating in the DSC can be used to initiate reordering of the non-equilibrium disordered structure, with the DSC results suggesting such a transition might occur between 530 to 740 °C. Based on the thermodynamic assessment of the Ni-Ge system given by Jin *et al*. [23] we estimate the enthalpy of formation for the ordered β-Ni_3Ge solid from the disordered solid to be ΔH = -1642 J mol^{-1} (6600 J kg^{-1}). Accordingly, the signal detected at 530 °C, being of the order of 0.1 mW from a typical 5 mg DSC sample, looks to be of appropriate magnitude given that the sample will only be partially disordered (all of the 'featureless' matrix is assumed fully ordered). Moreover, this result also indicated that the reaction is non-reversible, i.e. there is a transformation upon the first heating cycle (green arrow) which is not replicated on the second heating cycle (purple arrow). The most likely explanation for this is that the partially disordered material has undergone ordering at elevated temperature. Once ordered it then remains ordered. This differs from say the Ni_5Ge_3 intermetallic in the same system, in which thermal analysis indicated a reversible reaction upon re-heating/cooling [23].

Summary & conclusion

The congruently melting, single phase, intermetallic compound β-Ni_3Ge was subject to rapid solidification via drop-tube processing. Following drop-tube processing, the material remained as single phase β-Ni_3Ge, irrespective of the imposed cooling rate. Droplets

spanning the size range ≥ 850 to ≤ 38 μm, with equivalent cooling rates of ≤ 700 to > 54500 K s^{-1}, were subject to microstructural study by SEM. Six dominant solidification morphologies were identified, specifically; (i) spherulites, (ii) mixed spherulites and dendrites, (iii) dendrites – (orthogonal side-branching), (iv) dendrites – (non-orthogonal side branching), (v) recrystallised, and (vi) dendritic seaweed. In each case these features are observed embedded within a featureless matrix. SAD in the TEM analysis confirmed that it is only the spherulite microstructure that is partially ordered amongst the above listed microstructures, which are disordered. However, SAD analysis indicated that the featureless background material of all above microstructures is chemically ordered. Thermal analysis indicate a non-reversible reaction, which is differing than another Ni-Ge congruent melting intermetallic compound (Ni_5Ge_3).

Acknowledgments

The authors acknowledged financial support from Higher Education Commission (HEC) Pakistan and NED University of Engineering & Technology.

Conflict of interest

The authors declare they have no conflict of interest related to this work.

References

[1] J Magill (2001) Journal of materials science 36: 3143.

[2] L Gránásy, T Pusztai, G Tegze, JA Warren, JF Douglas (2005) Physical Review E 72: 011605.

[3] K Ziewiec (2005) Journal of alloys and compounds 397: 207.

[4] K Chrissafis, M Maragakis, K Efthimiadis, E Polychroniadis (2005) Journal of alloys and compounds 386: 165.

[5] T Yano, Y Yorikado, Y Akeno (2005) Materials transactions 46: 2886.

[6] C Xia, L Xing, W-Y Long, Z-Y Li, Y Li (2009) Journal of Alloys and Compounds 484: 698.

[7] J Liu, H Zhang, H Fu, Z-Q Hu, X Yuan (2010) Journal of Materials Research 25: 1159.

[8] H Sun, KM Flores (2011) Intermetallics 19: 1538.

[9] H Sun, KM Flores (2013) Intermetallics 43: 53.

[10] H Keith, F Padden Jr (1963) Journal of Applied Physics 34: 2409.

[11] HW Morse, CH Warren, JDH Donnay (1932) American Journal of Science: 421.

[12] A Nash, P Nash (1976) US National Bureau of Standards Monograph Series 25Elsevier, ASM, Ohio

[13] N Haque, RF Cochrane, AM Mullis (2016) Intermetallics 76: 70.

[14] N Haque, RF Cochrane, AM Mullis (2017) Metallurgical and Materials Transactions A 48: 5424.

[15] R Ahmad, R Cochrane, A Mullis (2012) Journal of Materials Science 47: 2411.

[16] A Nash, P Nash (1987) Journal of Phase Equilibria 8: 255.

[17] N Haque, RF Cochrane, AM Mullis (2017) Crystals 7: 100.

[18] N Haque, RF Cochrane, AM Mullis (2017) Journal of Alloys and Compounds 707: 327.

[19] R Ahmad, R Cochrane, A Mullis (2012) Journal of Materials Science 47: 2411.

[20] EG Castle, AM Mullis, RF Cochrane (2014) Acta Materialia 77: 76.

[21] K Dragnevski, R Cochrane, A Mullis (2002) Physical review letters 89: 215502.

[22] EG Castle, AM Mullis, RF Cochrane (2014) Acta Materialia 66: 378.

[23] N Haque, RF Cochrane, AM Mullis (2018) Journal of Alloys and Compounds 739: 160.